

## Development of terahertz laser diagnostics for electron density measurements<sup>a)</sup>

K. Kawahata,<sup>1,b)</sup> T. Akiyama,<sup>1</sup> K. Tanaka,<sup>1</sup> K. Nakayama,<sup>2</sup> and S. Okajima<sup>2</sup>

<sup>1</sup>National Institute for Fusion Science, Toki 509-5292, Japan

<sup>2</sup>Chubu University, Kasugai 487-8501 Japan

(Presented 13 May 2008; received 9 May 2008; accepted 25 July 2008;

published online 31 October 2008)

A two color laser interferometer using terahertz laser sources is under development for high performance operation on the large helical device and for future burning plasma experiments such as ITER. Through investigation of terahertz laser sources, we have achieved high power simultaneous oscillations at 57.2 and 47.6  $\mu\text{m}$  of a  $\text{CH}_3\text{OD}$  laser pumped by a cw 9R(8)  $\text{CO}_2$  laser line. The laser wavelength around 50  $\mu\text{m}$  is the optimum value for future fusion devices from the consideration of the beam refraction effect and signal-to-noise ratio for an expected phase shift due to plasma. In this article, recent progress of the terahertz laser diagnostics, especially in mechanical vibration compensation by using a two color laser operation and terahertz laser beam transmission through a dielectric waveguide, will be presented. © 2008 American Institute of Physics.

[DOI: [10.1063/1.2971976](https://doi.org/10.1063/1.2971976)]

### I. INTRODUCTION

Over the past ten years much progress has been made in magnetically confined devices for the improvement of plasma performance. In the large helical device,<sup>1</sup> we have successfully achieved superhigh density plasmas of over  $10^{21} \text{ m}^{-3}$ , so-called SDC plasmas,<sup>2</sup> which were achieved by the formation of a transport barrier created by the combination of repetitive pellet injection and a local island divertor pumping system. In these high density plasmas we observe fringe jumps on the density traces measured by a 118.8  $\mu\text{m}$   $\text{CH}_3\text{OH}$  laser interferometer<sup>3</sup> operating in LHD. In order to solve these difficulties we have been developing terahertz laser diagnostics<sup>4,5</sup> around 50  $\mu\text{m}$ . In these short wavelength laser diagnostics it is a critical issue how to compensate the effects of the mechanical vibrations on the interferometer, since the fringe shift caused by the mechanical vibrations is inversely proportional to the laser wavelength. In order to solve this problem the most convenient way is the application of a two color laser interferometer.<sup>6-8</sup> However, the conventional two color interferometer consists of two independent laser interferometers in general. In this type of the two color system, a fringe shift caused by the mechanical vibrations cannot be canceled out ideally since the optical path difference between the two interferometers remains and the effect of optically dispersive components (such as beam splitters/combiners or windows) are significant when the wavelengths of the two laser lights differ significantly. In order to overcome these difficulties, new types of two color laser interferometers have been developed<sup>9,10</sup> to establish more reliable vibration compensations. We have been developing a two color laser interferometer<sup>11</sup> in the terahertz range, using simultaneous oscillations at 57.2 and 47.6  $\mu\text{m}$

of a  $\text{CH}_3\text{OD}$  laser<sup>5</sup> optically pumped by the 9R(8)  $\text{CO}_2$  laser line. In this two color system, both laser beams pass the same optical path in the interferometer without any optical path difference. Moreover, the wavelength around 50  $\mu\text{m}$  is resistive to the darkening of vacuum windows and mirrors compared to visible and IR wavelength. This article reports recent progress of the diagnostic system, especially in mechanical vibration compensation and terahertz laser beam transmission.

### II. TWO COLOR LASER INTERFEROMETER

Figure 1 shows a schematic drawing of the two color laser interferometer system that is presently being tested. The system consists of a twin terahertz laser having a 3 m cavity length, beam splitters, beam combiners, a laser power monitoring system, and gallium-doped germanium photoconductors operating at the liquid He temperature. For the optical

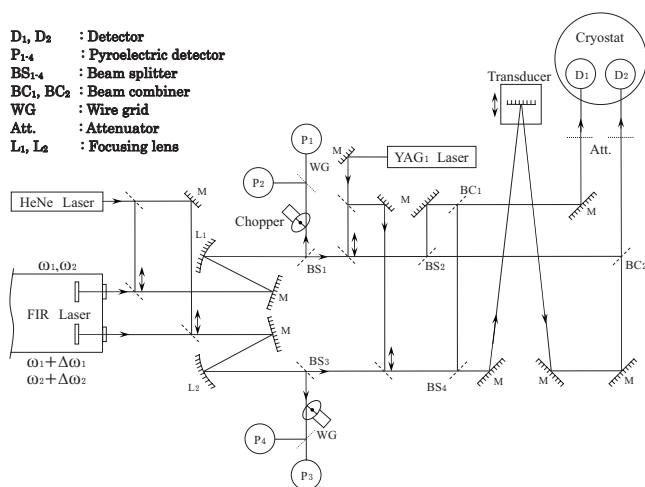


FIG. 1. Schematic drawing of a two color laser interferometer under development.

<sup>a)</sup> Contributed paper, published as part of the Proceedings of the 17th Topical Conference on High-Temperature Plasma Diagnostics, Albuquerque, New Mexico, May 2008.

<sup>b)</sup> Electronic mail: [kawahata@lhd.nifs.ac.jp](mailto:kawahata@lhd.nifs.ac.jp).

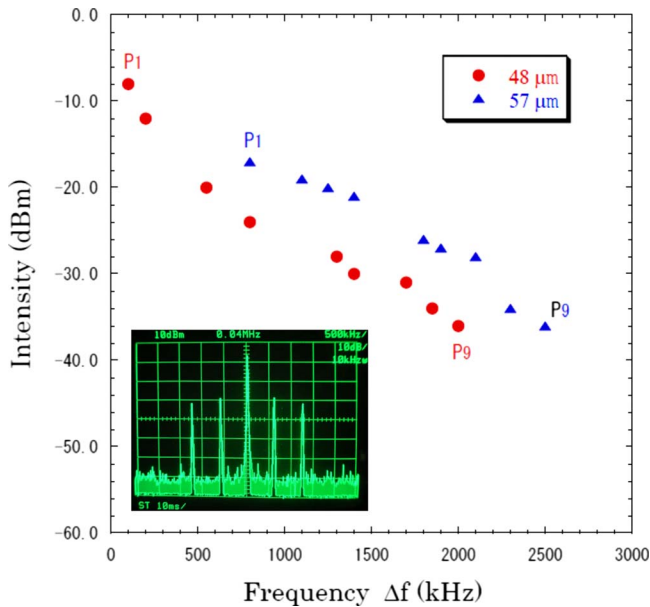


FIG. 2. (Color online) Intermediate signal levels of a 57.2  $\mu\text{m}$  laser and a 47.6  $\mu\text{m}$  laser as a function of frequency shift, and typical probe signal power spectrum showing two color beat frequencies (as inset). These beat frequencies are obtained by changing the cavity length ( $P_1$ – $P_9$ ).

axis alignment, both a visible He–Ne and a 1.06  $\mu\text{m}$  yttrium aluminum garnet (YAG) lasers are used since the beam splitters ( $\text{BS}_{1-4}$ ) and combiners ( $\text{BC}_1$ ,  $\text{BC}_2$ ) are made of non-doped silicon which is a low absorption material<sup>12</sup> in terahertz wavelength, but opaque to visible light. The optical axis of the terahertz laser is measured by using a liquid crystal sheet, and then the axis of a helium-neon laser is set on that of terahertz laser. After the beam splitters ( $\text{BS}_1$ ,  $\text{BS}_3$ ) optical components are aligned with a 1.06  $\mu\text{m}$  YAG laser with infrared sensor cards. The detectors are specially designed unstressed Ge:Ga detectors by QMC Instrument Ltd. for the improvement of the spectral responsivity around 50  $\mu\text{m}$ . The output power of each laser oscillation ( $\omega_1$ ,  $\omega_2$ ,  $\omega_1 + \Delta\omega_1$ ,  $\omega_2 + \Delta\omega_2$ ) is monitored by using pyroelectric detectors ( $P_{1-4}$ ) with mechanical choppers.

The beat frequencies can be changed with the cavity length and pressure of the far-infrared laser cavity. It is im-

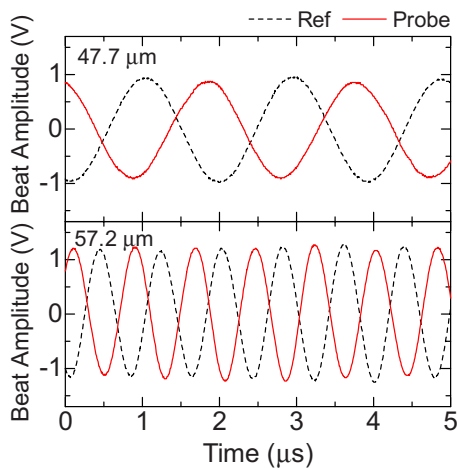


FIG. 3. (Color online) Two color beat signals detected by gallium-doped germanium photoconductors after bandpass frequency filtering.

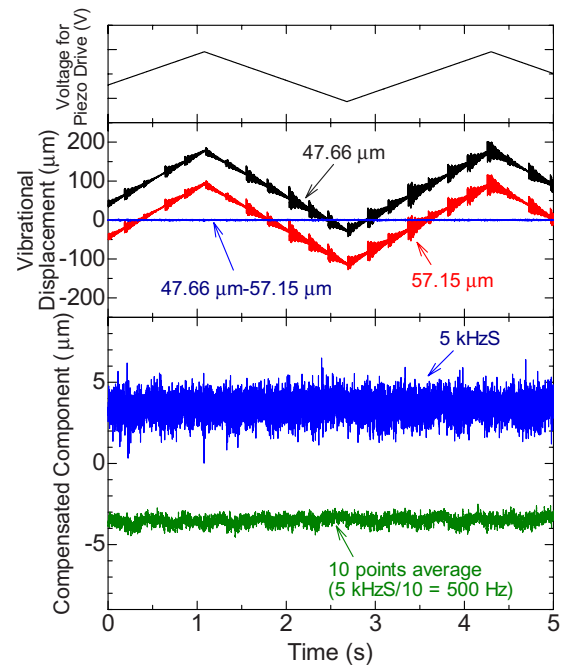


FIG. 4. (Color online) Typical experimental results from the two color laser interferometer. (a) Waveform of the applied voltage on the piezoelectric transducer. (b) The measured displacements of the vibration mirror by a 57.2 and 47.6  $\mu\text{m}$   $\text{CH}_3\text{OD}$  laser interferometer. (c) Expanded scale plots of the vibration compensation after low pass filtering. The mechanical vibration is simulated by using a piezoelectric transducer.

portant to know how high a beat frequency is available since the larger frequency modulation enables us to measure the electron density with a higher time resolution. Figure 2 shows intermediate frequency (IF) signal levels of two color laser oscillations as a function of frequency shift  $\Delta f$  (i.e., beat frequency). Here, the frequency shift is obtained by changing the length of one laser cavity of the twin laser system via stepping motor with a minimum step size of 0.02  $\mu\text{m}$ , while that of another laser cavity is fixed. The minimum step value of the frequency shift  $\Delta f$  can be calculated by simply using the tuning equation as follows:

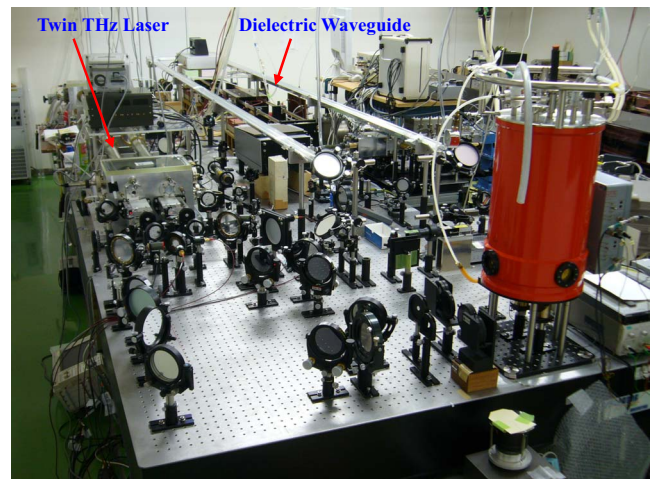


FIG. 5. (Color online) Laser beam transmission test stand composing of a hollow dielectric waveguide made of acrylic resin tube of 24 mm inner diameter and two miter bends.

$$\Delta f = -f \frac{\Delta L}{L}, \quad (1)$$

where  $f$  is the lasing frequency,  $L$  is the cavity length, and  $\Delta L$  is the fractional change in  $L$ . The beat frequency can be controlled with the accuracy of  $\sim 35$  kHz for  $57 \mu\text{m}$ . The noise level of the detection system including detector noise and laser noise is found to be about  $-60$  dBm, which is seen on a frequency spectrum inserted in Fig. 2. Each beat frequency moves simultaneously with the laser cavity length, for instance, from 0.1 MHz ( $48 \mu\text{m}$ ) and 0.8 MHz ( $57 \mu\text{m}$ ) to 2.0 MHz ( $48 \mu\text{m}$ ) and 2.5 MHz ( $57 \mu\text{m}$ ). The detected IF signal gradually decreases with the frequency shift  $\Delta f$  and

then strongly at frequencies over 1.5 MHz. The reduction in IF signal level in the high frequency region of over than 1.5 MHz is mainly caused by the response of the preamplifiers (QMC Instrument Ltd., ULN95) having a 3 dB frequency bandwidth of 1.5 MHz. In a test bench experiment, the beat frequencies are set at  $\sim 0.5$  MHz ( $48 \mu\text{m}$ ) and  $\sim 1.2$  MHz ( $57 \mu\text{m}$ ), which gives the signal-to-noise ratio (S/N) of  $\sim 40$  dB. This adequate S/N is achieved when the input power to the detector is reduced by 30 dB and the input power level of each laser line is adjusted to be the same.

Figure 3 shows the two color IF signals detected after passing through IF bandpass filters, which have 3 dB frequency bandwidths of 300–900 kHz and 1.1–1.7 MHz, re-

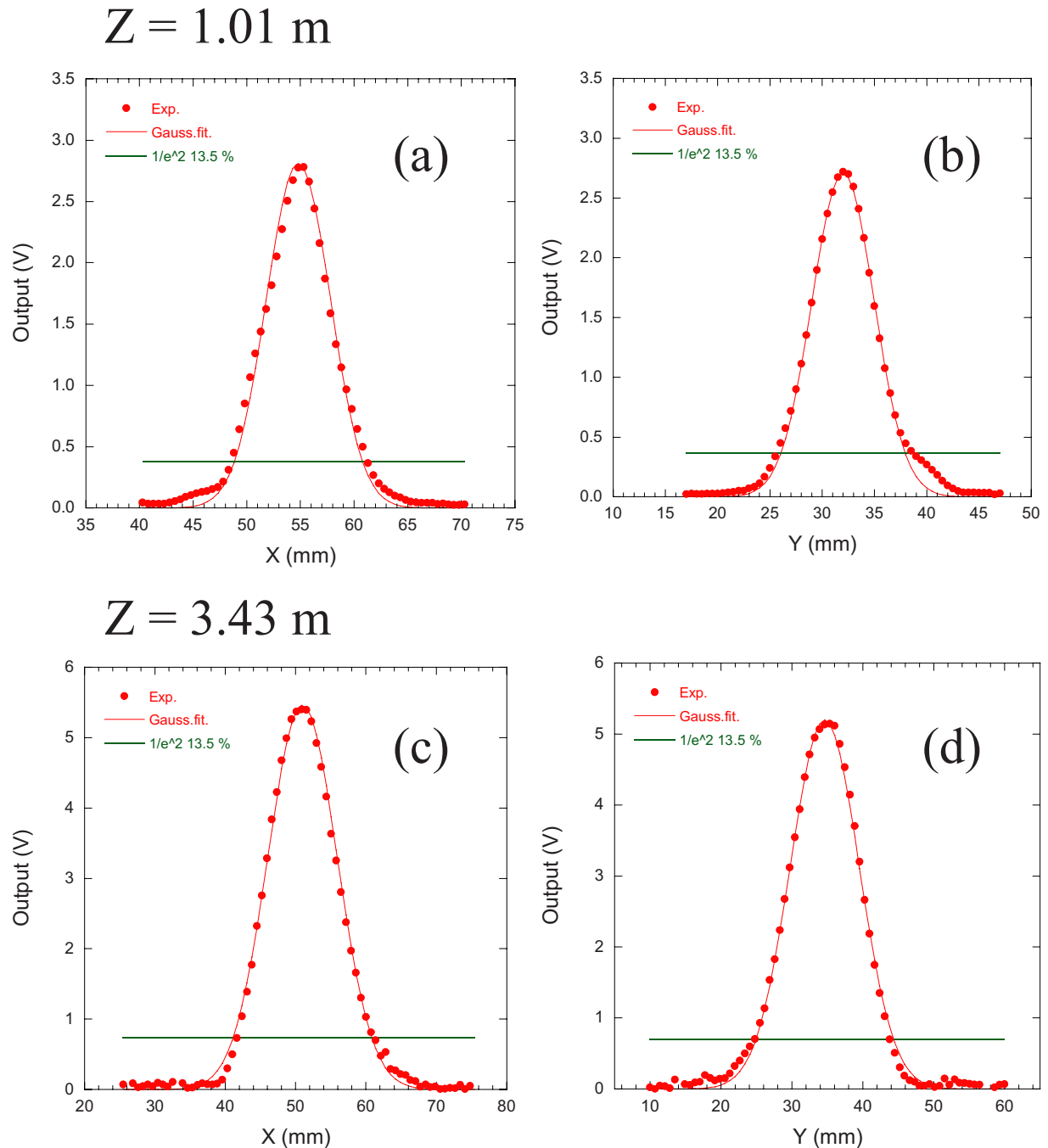


FIG. 6. (Color online) Horizontal and vertical mode profiles of a  $57.2 \mu\text{m}$  laser beam after passing through the dielectric waveguide of 8.9 m in length. (a) and (b) measured at a distance of 1.01 m from the end of the waveguide. (c) and (d) measured at a distance of 3.43 m.

spectively. These IF signals are introduced into phase comparators for phase measurements. In order to simulate mechanical vibration, a reflecting mirror was modulated by means of a piezoelectric transducer, and the mirror holder was shocked mechanically to give high frequency mechanical vibrations. Figure 4 shows that the low ( $\sim 0.3$  Hz with the amplitude of  $100 \mu\text{m}$ ) and high frequency ( $\sim 140$  Hz with the amplitude of  $\sim 26 \mu\text{m}$ ) components of the phase shifts caused by mechanical vibrations were canceled out completely. In Fig. 4(c) the same measurement of the compensated components is shown with an expanded scale. Both the low and high frequency components of the phase shift cannot be seen on the traces. In the present situation, an uncompensated error after vibration compensation is less than  $0.3 \mu\text{m}$ . The standard deviation of the high frequency phase noise of the system observed in Fig. 4(c), which is thought to be due to detector noise or laser oscillation noise, corresponds to the mechanical vibration amplitude of  $0.63 \mu\text{m}$ . Since the fundamental function of the two color interferometer, vibration subtraction, was confirmed, this diagnostic system will be upgraded to the combined system with polarimetry in near future.

### III. LASER BEAM PROPAGATION TEST IN A DIELECTRIC WAVEGUIDE

In large fusion devices, a laser diagnostic system should be located behind a biological shield to avoid radiation effects on the laser and detection system and to allow laser maintenance easily, so that the laser beam has to travel a long distance to reach a fusion device, for instance, 44 m in the case of ITER. There are two ways of laser beam propagation, free space propagation and waveguide propagation. Waveguide propagation has been applied to many large fusion devices such as JET, LHD, and so on, since a waveguide system has precise mode matching, easy alignment and is less sensitive<sup>13</sup> to the change in the incident angle. However, there is no experience on waveguide transmission of terahertz lasers, therefore we constructed a dielectric waveguide system with two miter bends as is shown in Fig. 5. The waveguide system has total length of  $\sim 9$  m and is filled with dry air in order to reduce absorption of the  $\text{CH}_3\text{OD}$  laser radiation by atmospheric water vapor. The attenuation coefficient measured at the wavelength of  $57 \mu\text{m}$  is about  $-3.8$  dB/m at the relative humidity of 50%.

The laser beam is introduced into an oversized dielectric waveguide (acrylic resin tube of 24 mm inner diameter) by using a concave mirror (focal length: 1885 mm). With this test stand we have confirmed the stability of the beam axis, mode properties emerging from the waveguide, and transmission efficiency of the waveguide. Figure 6 shows horizontal and vertical mode qualities of a  $57.2 \mu\text{m}$  laser beam, which were measured at 1.01 and 3.43 m from the end of the waveguide. Beam profile is measured with the combination of a motorized two-dimensional stage and a pyroelectric detector. The measured intensity distributions are well fitted by normalized Gaussian beam profiles expressed as  $\exp(-4x^2/d^2)$ , where  $x$  is the distance from the axis and  $d$  is the diameter at the  $1/e$  point of the intensity profile. The

diameter at the beam waist can be estimated by using Gaussian beam propagation, and corresponds to a waist diameter of 12.2 mm. This value is a bit smaller than a width of  $1/e$  of 13.4 mm for the  $J_0(x)$  distribution of the  $\text{EH}_{11}$  mode of the waveguide. This discrepancy may be due to the transition from the Bessel function distribution to the Gaussian mode.

The stability of the laser beam optical axis is important for establishment of reliable laser diagnostics. In order to investigate effects caused by the misalignment or change in the coupling mirror on the laser beam propagation, the incident angle to the waveguide is changed by tilting the facing mirror located at 930 mm from the input of the waveguide. By tilting the incident mirror, the measured profile peak value decreases and its position slightly shifts from the optical axis, and an additional propagation mode appears (a side-lobe clearly appears in addition to the main lobe) when the incident angle is larger than 1.8 mrad. It is a bit hard to estimate the stability of a real transmission system, but sufficient stability of waveguide transmission for a long time has already been confirmed in the LHD laser interferometer system,<sup>3</sup> where a 40 m long dielectric waveguide system including five miter bends has been applied. The laser power is measured by using the power meter Vector H310 (Sciencetech, Inc.) before and after waveguide transmission, and it is found that the transmission efficiency measured is over 90%.

### ACKNOWLEDGMENTS

The authors would like to thank Professor S. Sudo and Professor O. Motojima for their encouragement. This work was supported in part by a Grant-in-Aid for Science Research from the Japanese Ministry of Education, Culture, Sports, Science and Technology, "Priority area of Advanced Burning Plasma Diagnostics" (No. 16082208) and also by the NIFS budget code of NIFS06ULHH501.

- <sup>1</sup>O. Motojima, N. Ohya, A. Komori, O. Kaneko, H. Yamada, K. Kawahata, Y. Nakamura, K. Ida, T. Akiyama, N. Ashikawa, *et al.*, *Nucl. Fusion* **43**, 1674 (2003).
- <sup>2</sup>N. Ohya, T. Morisaki, S. Masuzaki, R. Sakamoto, M. Kobayashi, J. Miyazawa, M. Shoji, A. Komori, and O. Motojima, *Phys. Rev. Lett.* **97**, 055002 (2006).
- <sup>3</sup>K. Kawahata, K. Tanaka, Y. Ito, A. Ejiri, and S. Okajima, *Rev. Sci. Instrum.* **70**, 707 (1999).
- <sup>4</sup>S. Okajima, K. Nakayama, H. Tazawa, K. Kawahata, K. Tanaka, T. Tokuzawa, Y. Ito, and K. Mizuno, *Rev. Sci. Instrum.* **72**, 1094 (2001).
- <sup>5</sup>K. Nakayama, H. Tazawa, S. Okajima, K. Kawahata, K. Tanaka, T. Tokuzawa, and Y. Ito, *Rev. Sci. Instrum.* **75**, 329 (2004).
- <sup>6</sup>I. H. Irby, E. S. Marmor, E. Sevillano, and S. M. Wolfe, *Rev. Sci. Instrum.* **59**, 1568 (1988).
- <sup>7</sup>Y. Kawano, A. Nagashima, T. Hatae, and S. Gunjiawahata, *Rev. Sci. Instrum.* **67**, 1520 (1996).
- <sup>8</sup>G. Braithwaite, N. Gottardi, G. Magyar, J. O'Rourke, J. Ryan, and D. Vernon, *Rev. Sci. Instrum.* **60**, 2825 (1989).
- <sup>9</sup>J. Irby, R. Murray, P. Acedo, and H. Lamela, *Rev. Sci. Instrum.* **70**, 699 (1999).
- <sup>10</sup>P. A. Bagryansky, A. D. Khilchenko, A. N. Kvashnin, A. A. Lizunov, R. V. Voskovoynikov, A. L. Solomakhin, H. R. Koslowski, and TEXTOR team, *Rev. Sci. Instrum.* **77**, 053501 (2006).
- <sup>11</sup>K. Kawahata, T. Akiyama, R. Pavlichenko, K. Tanaka, T. Tokuzawa, Y. Ito, S. Okajima, K. Nakayama, and K. Wood, *Rev. Sci. Instrum.* **77**, 10F132 (2006).
- <sup>12</sup>K. Nakayama, H. Tazawa, S. Okajima, K. Kawahata, K. Tanaka, T. Tokuzawa, and Y. Ito, *Electr. Eng. Jpn.* **153**, 1 (2005).
- <sup>13</sup>J. P. Crenn, *IEEE Trans. Microwave Theory Tech.* **27**, 573 (1979).